



OPEN

A composite patch loaded with 2-Deoxy Glucose facilitates cardiac recovery after myocardial infarction via attenuating local inflammatory response

Weizhang Xiao¹, Zhen Zhu¹, Zhiming Yu¹, Yue Pan¹, Qun Xue¹, Youlang Zhou² & Jiahai Shi¹

Local inflammatory microenvironment in the early stage of myocardial infarction (MI) severely impaired cardiac recovery post-MI. Macrophages play a pivotal role in this process. A classical glycolytic inhibitor, 2-Deoxy-Glucose (2-DG), has been found to regulate the excessive pro-inflammatory macrophage polarization in the infarcted myocardium. This study investigated the effect of 2-DG-loaded chitosan/gelatin composite patch on the infarct microenvironment post-MI and its impact on cardiac repair. The results showed that the 2-DG patch significantly inhibited the expression of inflammatory cytokines, alleviated reactive oxygen species (ROS) accumulation, repressed the proinflammatory polarization of macrophages, attenuated local inflammatory microenvironment in the ischemic hearts, as well as improved cardiac function, reduced scar size, and promoted angiogenesis post-MI. In terms of mechanism, 2-DG exerts anti-inflammatory effects through inhibiting the NF- κ B signaling pathway and reducing the assembly and activation of the NLRP3 inflammasome. These findings suggest that 2-DG composite patch may represent a promising therapeutic strategy for cardiac repair after MI.

Keywords Myocardial infarction, Inflammatory microenvironment, Macrophage polarization, 2-deoxy-glucose, Glycolysis

Coronary heart disease (CHD), the underlying disease of most acute cardiac events, remains the leading cause of death worldwide¹. Myocardial infarction (MI) is the most common and severe manifestation of CHD, reportedly attacking one American every 40 s, and approximately 35% of those who have experienced an MI will die from it². Currently, the treatment of MI mainly focuses on rapid revascularization and reperfusion, including vasodilators, anticoagulants, stent implantation or bypass, as well as reducing the burden on hearts, such as β -blockers^{3–5}. In recent years, cardiac repair after MI has gained more attention, and increasing number of researches have explored the adverse effects of local inflammatory response on cardiac recovery^{6,7}.

After MI occurs, due to the reduction of oxygenated blood supply, anaerobic glycolysis occurs in the ischemic region, leading to the depletion of nutrients, accumulation of acidic metabolites and reactive oxygen species, extensive cell death and extracellular matrix degradation^{8,9}. The death cells and matrix fragments recruit neutrophils and mononuclear/macrophages through damage-associated molecular patterns (DAMPs), which further release a cascade of inflammatory cytokines, resulting in a harmful inflammatory microenvironment that severely impairs the cardiac recovery^{10,11}.

It has been established that mononuclear/macrophages orchestrate all stages of MI^{12,13}. In the inflammatory phase, Ly6C^{hi} monocytes are recruited to the infarcted area and differentiate into classically activated CCR⁺ or M1 macrophages, which play an essential role in the inflammatory microenvironment. About 5 days after MI, CCR⁻ or M2 macrophages with an anti-inflammatory phenotype gradually become dominant, indicating the arrival of reparative phase^{9,12}. Consistent with the biological behavior of M1 macrophages, their primary source of

¹Department of Cardiothoracic Surgery, Affiliated Hospital and Medical School of Nantong University, Nantong 226001, China. ²Research Center of Clinical Medicine, Affiliated Hospital of Nantong University, Nantong 226001, Jiangsu, China. ✉email: xwz191201@163.com; happysjh167@163.com

energy is rapid glycolysis¹⁴. Our previous studies have found that 2-deoxyglucose (2-DG), as a common inhibitor of glycolysis, can regulate macrophage polarization. Locally applied 2-DG-loaded chitosan/gelatin composite patch enhanced the therapeutic effect of stem cell transplantation on MI through promoting stem cell retention and survival¹⁵. However, whether application of 2-DG patch alone can also generate similarly positive impact on cardiac repair and its underlying mechanism remain unknown. Therefore, we attached the 2-DG patch directly onto the infarcted area and evaluated the improvement of the local inflammatory microenvironment in the ischemic hearts and subsequent cardiac repair.

Results

Inhibition of Glycolysis in Macrophages by 2-DG-CM

The morphology of 2-DG patch was shown in Fig. 1A,B. The patch exhibits a rugged appearance with an irregular fracture surface, displaying a jagged pattern. The sustained release of 2-DG patch has been demonstrated in our

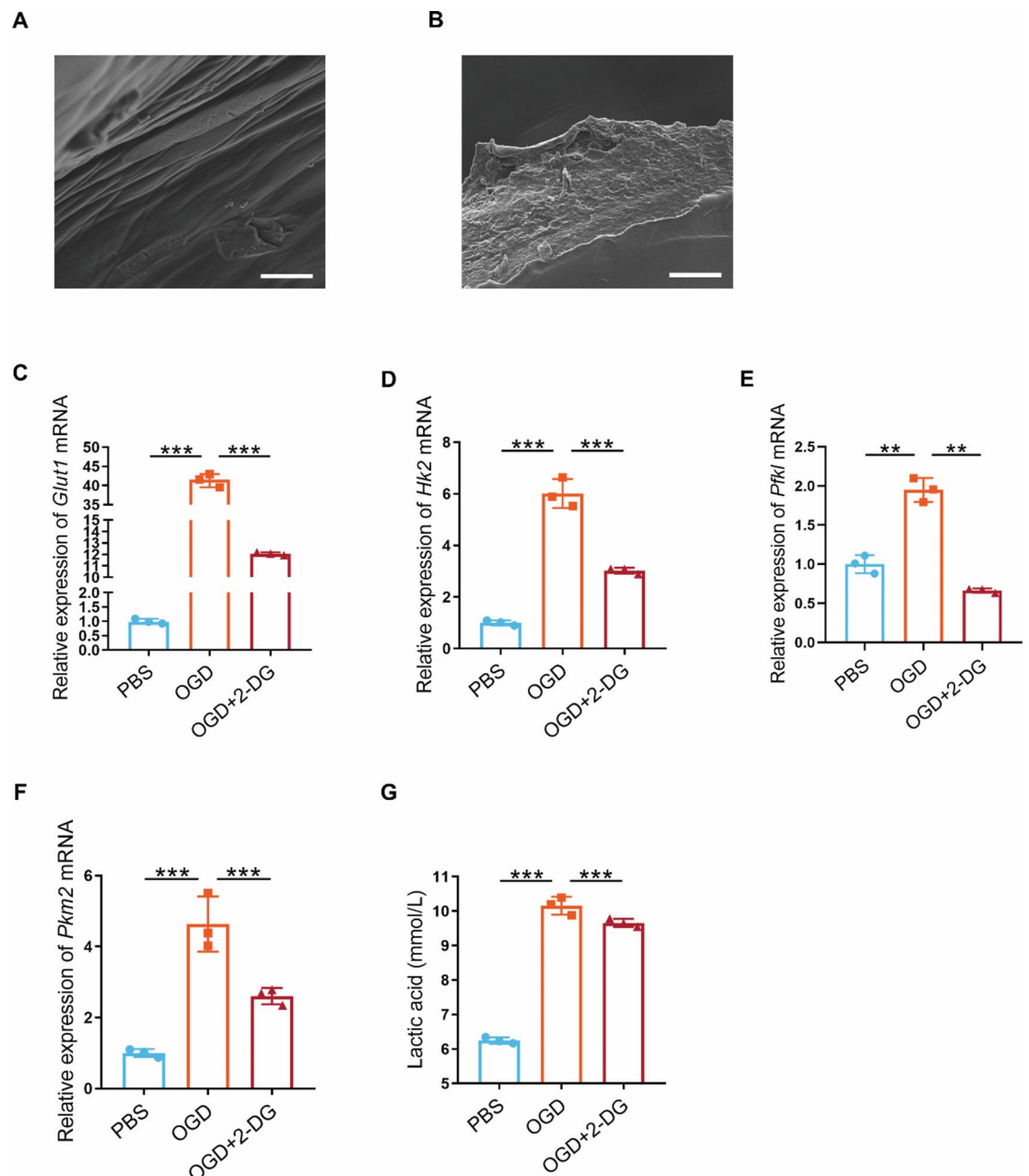


Fig. 1. 2-DG inhibits the glycolysis of macrophage under OGD. (A,B) Morphology of 2-DG patch using scanning electron microscopy. Scale bar, A, 25 μ m; B, 50 μ m. (C–F) Relative gene expression of *Glut1* (C), *Hk2* (D), *Pfkf* (E), and *Pkm2* (F) in macrophages under OGD with or without 2-DG pretreatment (n = 3). (G) Lactate production by macrophages in OGD condition with or without 2-DG pretreatment (n = 3). All data are presented as mean \pm SD, and significance was determined using one-way ANOVA followed by Tukey's test (**p < 0.01, and ***p < 0.001).

previous study¹⁵. Herein, we employed an OGD model to imitate the ischemic and hypoxic microenvironment in vivo and blocked the glycolysis with 2-DG-CM. Firstly, to disentangle whether macrophage polarization is linked to apoptosis, we conducted an apoptosis assay. The results indicated that neither OGD treatment alone nor OGD combined with 2-DG treatment led to an increase in macrophage apoptosis (Fig. S1). Subsequently, we examined the gene expression of glycolytic rate-limiting enzymes in macrophages. Notably, we found that the expression of glucose transporter 1 (Glut1), hexokinase 2 (Hk2), phosphofructokinase-1 liver type (PFKL), and pyruvate kinase isoform M2 (Pkm2) was upregulated in OGD environment, which was significantly reversed by 2-DG pretreatment (Fig. 1C–F). Additionally, the elevated lactate levels in the culture medium due to OGD treatment were notably reduced (Fig. 1G), indicating that 2-DG-CM can potentially inhibit glycolysis in macrophages under OGD conditions.

2-DG-CM compromises the proinflammatory polarization of macrophages

To investigate whether 2-DG-CM modulates the immunophenotypic switch of macrophages while blocking glycolysis under OGD conditions, we first examined the expression profile of pro-inflammatory cytokines. The results revealed that OGD triggered a notable increase in mRNA levels of canonical pro-inflammatory cytokines, including *Nos2*, *Il1b*, *Il6*, and *Tnfa* (Fig. 2A–D). Meanwhile, there was a marked elevation in iNOS protein levels (Fig. 2E,F), indicating a shift towards the pro-inflammatory phenotype. However, the preemptive blockade of glycolysis significantly attenuated this phenomenon. Furthermore, as illustrated by flow cytometry analysis, the proportion of iNOS-positive macrophages increased from 25.3% to 36.4% under OGD treatment, which was reduced to 28.7% by 2-DG-CM pre-treatment (Fig. 2G–H). Intriguingly, pretreatment of 2-DG-CM failed to modulate the CD206⁺ F4/80⁺ macrophages (Fig. S2A,B), which was consistent with a previous report regarding M1-M2 repolarization¹⁶. Concurrently, immunofluorescence staining demonstrated a significant decrease in the fluorescence intensity of iNOS (Fig. 2I,J). The findings delve deeply into the role of 2-DG-CM in the immune modulation of macrophage.

2-DG patch facilitates cardiac repair after MI

Next, to explore whether 2-DG patch positively contributes to cardiac repair, we attached the composite patch to the infarcted area immediately after LAD ligation, then the continuous echocardiography was employed to assess cardiac function. As illustrated in Fig. 3A–D and Fig. S3, a dramatically declined myocardial function was observed following MI. Notably, compared to the MI group, mice in the MI + 2-DG patch group exhibited superior left ventricular ejection fraction (LVEF) and fractional shortening (LVFS) on both 14- (LVEF: 28.40% ± 5.61% vs. 21.05% ± 3.66%, $p < 0.01$; LVFS: 13.21% ± 2.91% vs. 9.58% ± 1.72%, $p < 0.01$) and 28-days (LVEF: 30.38% ± 5.13% vs. 20.89% ± 2.50%, $p < 0.001$; LVFS: 14.03% ± 2.45% vs. 9.50% ± 1.24%, $p < 0.001$) post-MI. In contrast, mice receiving single patch treatment without 2-DG failed to demonstrate any improvement in cardiac recovery. Furthermore, the fibrotic area was evaluated using Masson's trichrome staining, and the results disclosed a reduced scar size in 2-DG patch group (Fig. 3E,F). Besides, the MI-induced collagen deposition in the infarct border area was significantly inhibited by 2-DG patch (Fig. 3G,H). Additionally, an increased capillary density within the infarcted region was observed in mice treated with 2-DG patch (Fig. 3I,J). Collectively, these findings suggest that 2-DG patch could facilitate cardiac recover after MI, which is attributed to the sustained release of 2-DG, rather than the patch itself.

Glycolysis inhibition protects against inflammatory response in infarcted hearts

Given that the patch alone does not benefit cardiac repair, the single patch group was omitted from the subsequent experiments. To explore whether the composite patch could alleviate inflammatory stress in the ischemic myocardium as anticipated, the infarcted hearts of mice were harvested on the 3rd day post-MI, when the inflammatory storm culminated. Firstly, RT-PCR analysis revealed that the 2-DG patch suppressed the expression of glycolytic rate-limiting enzymes in the infarcted myocardium, indicating effective glycolytic inhibition by the sustained release of 2-DG from the patch (Fig. 4A–D). Subsequently, the inflammatory cytokines at both the gene and protein levels were dramatically upregulated in the infarcted hearts, which was attenuated by the 2-DG patch (Fig. 4E–J). Additionally, given the crucial role of oxidative stress in inflammatory responses in the infarct zone, we utilized the DHE probe and found that the 2-DG patch significantly decreased ROS production in the ischemic area (Fig. 4L–M). Collectively, 2-DG patch can attenuate inflammatory response in the infarcted myocardium by suppressing glycolysis.

2-DG patch alleviated the infiltration of proinflammatory macrophages in infarcted myocardium

As previously mentioned, the infiltration of immune cells, including neutrophils and macrophages, plays a pivotal role in the early inflammatory response after MI. To assess the infiltration of these cells, the infarcted hearts were harvested, minced, and digested into single cell suspension on the 3rd day post-MI. As illustrated by flow cytometry, after MI, the percentage of neutrophils in the infarcted hearts increased from 1.66 ± 0.15% to 18.28 ± 2.63% (Fig. 5A,B). However, in the 2-DG patch group, this proportion was 16.3 ± 2.49%, revealing no statistically significant difference compared to the MI group. Similarly, there was no notable difference in the absolute neutrophil count, indicating that the application of 2-DG patch failed to reduce the neutrophil infiltration on the 3d day post-MI.

Subsequently, the accumulation of macrophages in the ischemic myocardium was explored. Firstly, infiltrated macrophages increased dramatically after MI, which was partly reversed by treatment of 2-DG patch (Fig. S4). Then, the subset of macrophages was investigated. As shown in Fig. 5C,D, both the ratio and number of iNOS⁺ macrophages were decreased in the 2-DG patch treated hearts. Consistent with the in vitro study, 2-DG patch

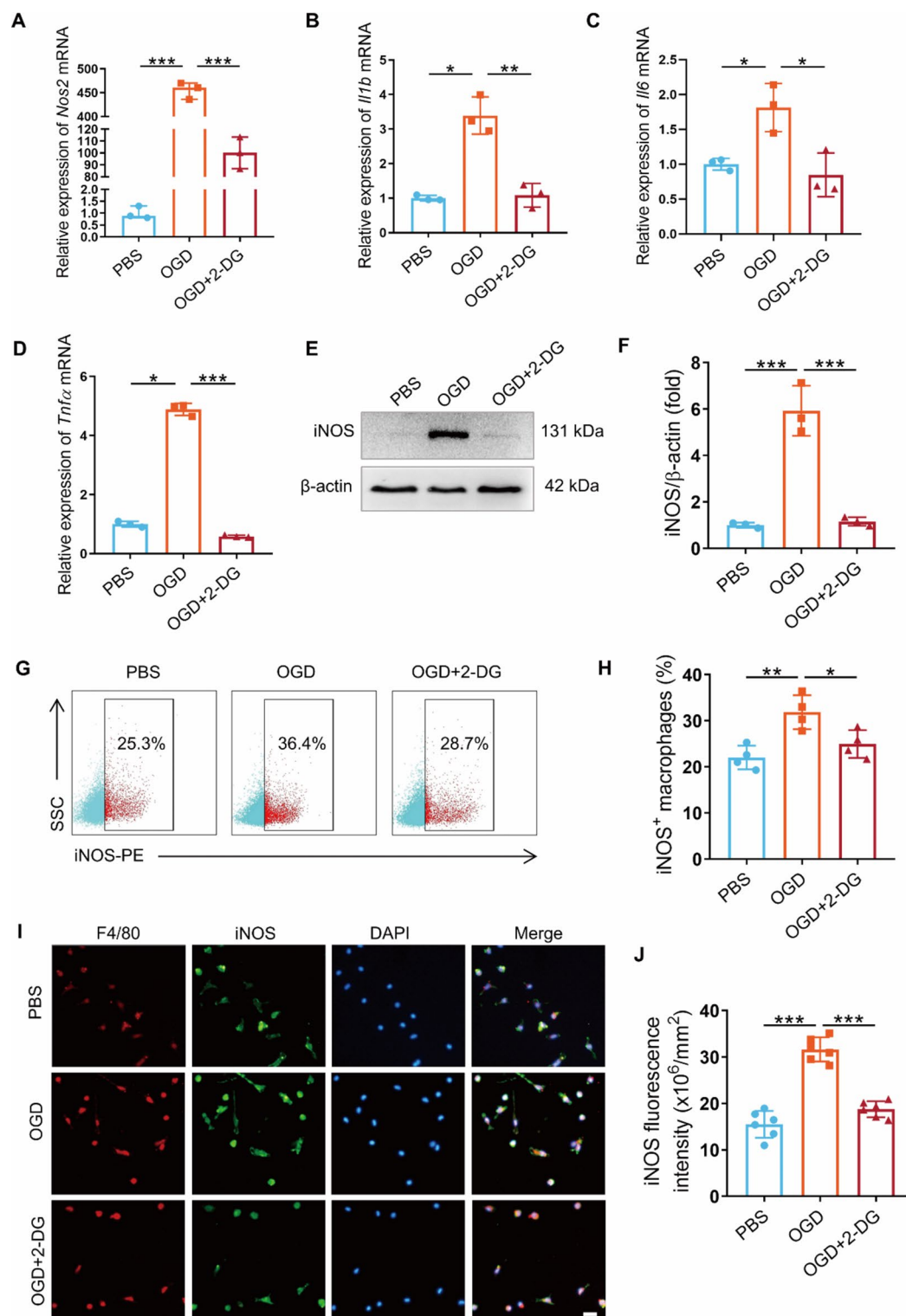


Fig. 2. Blockage of glycolysis compromises the proinflammatory polarization of macrophages. (A–D) Relative gene expression of *Nos2* (A), *Il1b* (B), *Il6* (C), and *Tnfa* (D) in macrophages under OGD with or without 2-DG pretreatment ($n = 3$). (E,F) The iNOS protein expression of macrophages under OGD \pm 2-DG (E) and the quantification of immunoblotting (F) ($n = 3$). Original blots/gels are presented in Supplementary Figure S5. (G,H) Representative flow cytometry analysis (G) and quantification (H) of the iNOS⁺ macrophages ($n = 4$). (I,J) Representative immunofluorescence images (I) and quantification of the iNOS (green) fluorescence intensity (J) ($n = 6$). Scale bar, 50 μ m. Error bars represent the SD, and significance was determined using one-way ANOVA followed by Tukey's test (* $p < 0.05$, ** $p < 0.01$, and *** $p < 0.001$).

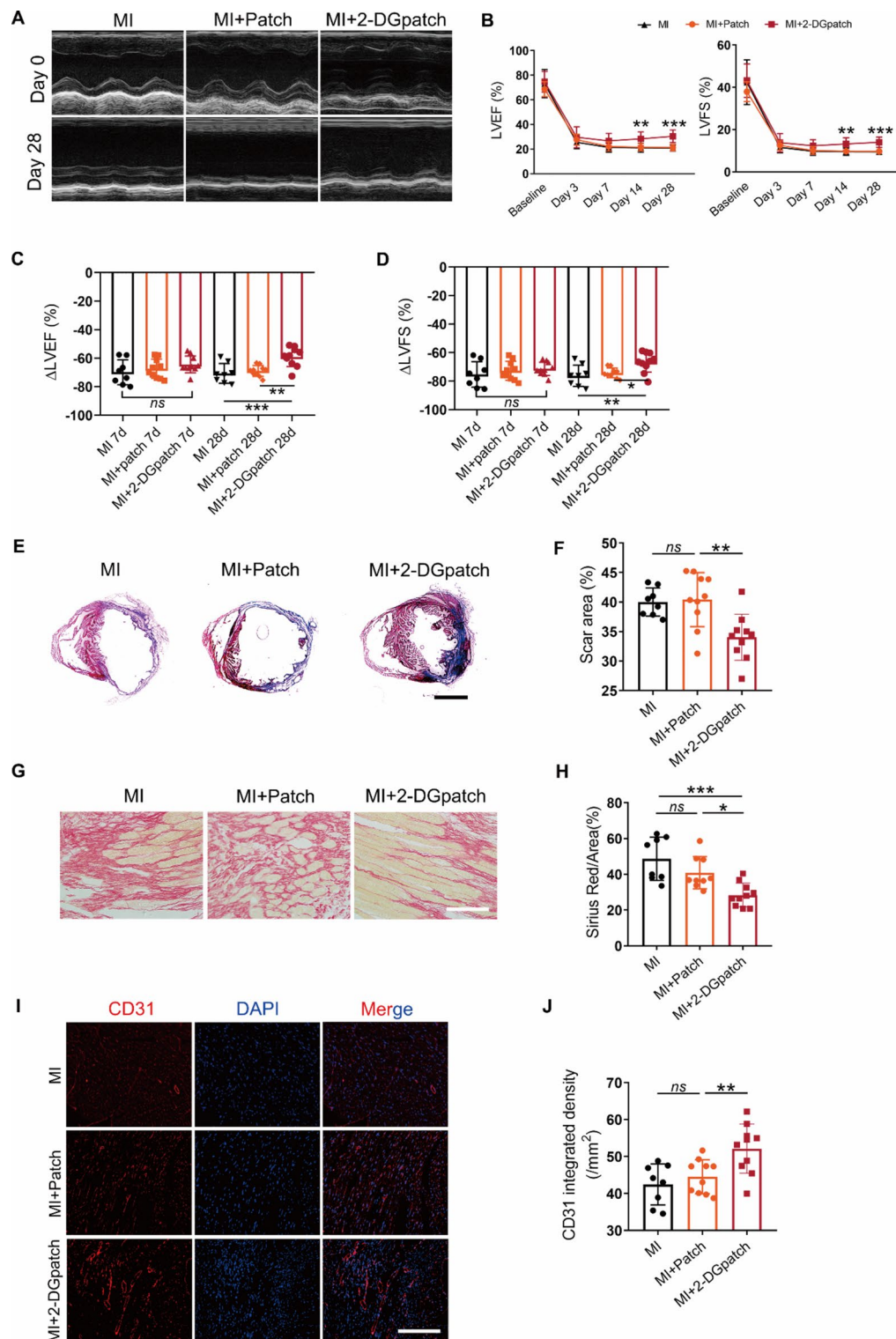


Fig. 3. The employment of 2-DG patch improves cardiac function in mice post-MI. (A) Representative M-mode short-axis echocardiography images of mouse hearts on Day 0 and Day 28 post-MI. (B) Quantitative analysis of LVEF and LVFS at baseline, day 0, day 3, day 7, day 14, and day 28 post-MI (n = 8–10). * for the comparison of MI+2-DGpatch group with MI group. (C,D) The reduction in LVEF (C) and LVFS (D) on day 7 and day 28 post-MI. (E) Representative images of Masson's trichrome-stained heart sections on Day 28 after surgery. Scale bar, 4 mm. (F) Quantification of the scar area (n = 8–10). (G,H) Representative images (G) and quantification (H) of collagen content in the infarct border zone with Sirius red staining (red) at day 28 post-MI. Scale bar, 500 μ m. n = 8–10, three independent sections per group. (I) Representative graphs of capillaries in the infarct zone detected with CD31 immunofluorescence staining (red) on Day 28 post-MI. Scale bar, 200 μ m. (J) Quantitative analysis of the capillary density (n = 8–10, three independent sections per group). Data are presented as the means \pm SD and were analyzed using one-way ANOVA followed by Tukey's test. LVEF and LVFS were analyzed using two-way ANOVA followed by Tukey's test (* p < 0.05, ** p < 0.01, *** p < 0.001, and *ns* for not significant).

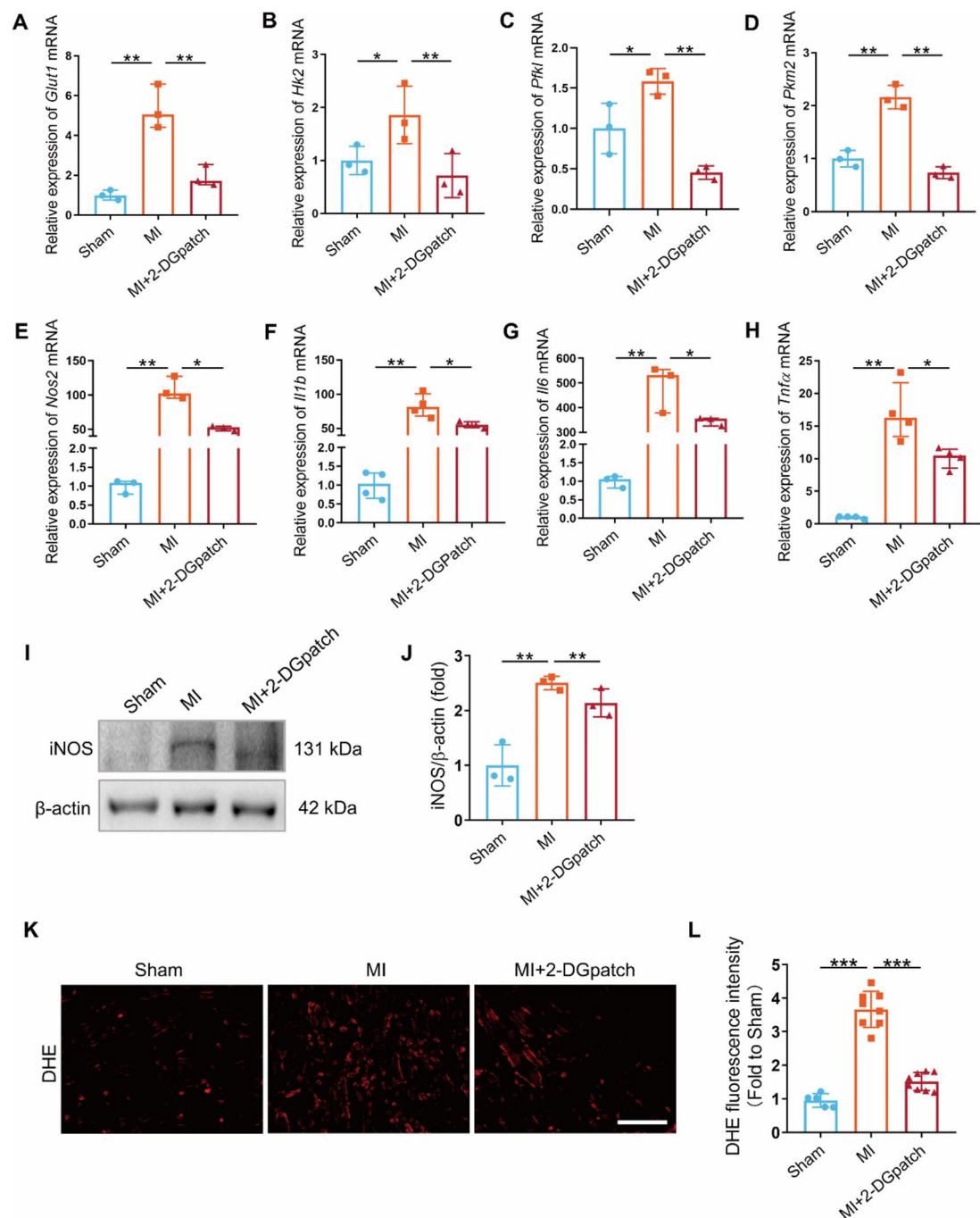


Fig. 4. Glycolytic inhibitor-loaded patch protects against local inflammatory response in infarcted hearts. (A–D) Relative gene expression of *Glut1* (A), *Hk2* (B), *Pfkf1* (C), and *Pkm2* (D) in myocardium (n = 3). (E,H) Relative gene expression of *Nos2* (E), *Il1b* (F), *Il6* (G), and *Tnfa* (H) in myocardium (n = 3). (I,J) Representative images (I) and quantification (J) of western blotting analysis of iNOS in infarcted hearts on Day 3 post-MI (n = 3). Original blots/gels are presented in Supplementary Figure S5. (K,L) Representative images (K) and quantification (L) of superoxide levels in ischemic myocardium using DHE staining at day 3 after MI (n = 5–8). Scale bar, 200 μ m. Error bars represent the SD, and significance was determined using one-way ANOVA followed by Tukey's test (*p < 0.05, **p < 0.01, and ***p < 0.001).

failed to modulate the anti-inflammatory CD206⁺ F4/80⁺ macrophages in the infarcted hearts (Fig. S2C,D). Moreover, the immunofluorescence staining revealed a marked enhancement of iNOS green signals in the infarcted area, which was partly reversed by the application of 2-DG patch, indicating an attenuated infiltration of M1 macrophages in the ischemic region (Fig. 5E,F).

Taken together, these findings suggest that 2-DG patch modulates the infiltration of proinflammatory macrophages, thereby suppressing the hyperinflammatory response in the infarcted area, which contributes to the ultimate cardiac recover.

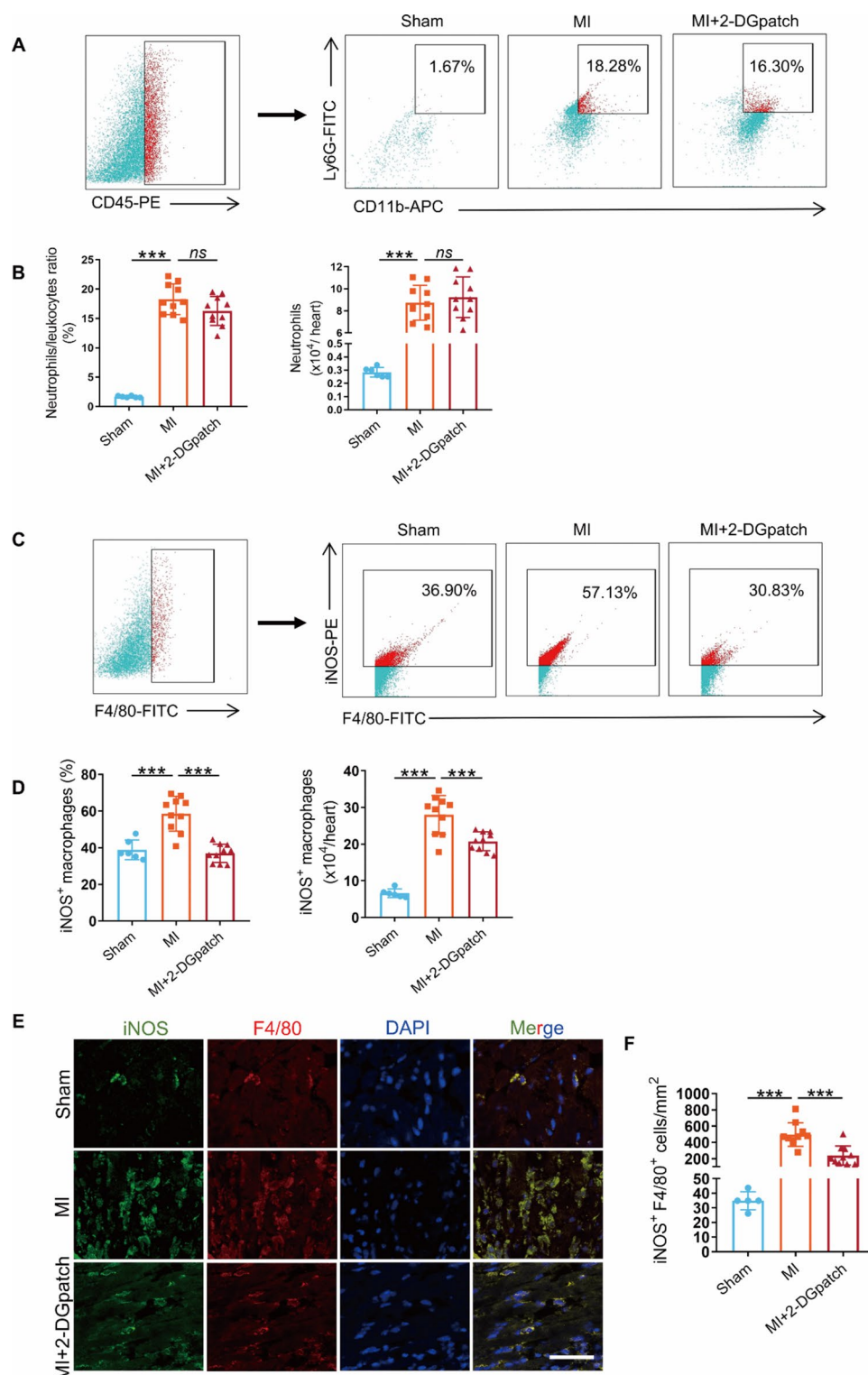


Fig. 5. Immune cells infiltration after MI. **(A,B)** Representative flow cytometry analysis **(A)** and quantification **(B)** of neutrophils in the infarcted hearts on Day 3 post-MI ($n = 6-10$). **(C,D)** Representative flow cytometry analysis **(C)** and quantification **(D)** of the iNOS⁺ macrophages in the infarcted hearts on Day 3 post-MI ($n = 6-10$). **(E,F)** Representative immunofluorescence images **(E)** and quantification **(F)** of the iNOS⁺F4/80⁺ cells in the ischemic myocardium at day 3 after MI ($n = 5-10$). Scale bar, 100 μm . Error bars represent SD and significance was determined by one-way ANOVA test (** $p < 0.001$, and ns for not significant).

2-DG inhibits the NF- κ B pathway and attenuates the activation of NLRP3

The oxidative stress and DAMPs resulting from myocardial ischemia have been demonstrated to trigger the activation of NF- κ B and the NLRP3 inflammasome, which occupies a pivotal position in the initial inflammatory response to MI^{17,18}. Therefore, we conducted in vitro experiments to investigate the effect of 2-DG on these biological processes. Western blot revealed that OGD upregulated the protein expression of NLRP3, HIF-1 α , Caspase-1, and pIkBa, while downregulated the IkBa expression (Fig. 6). However, 2-DG pretreatment partly reversed these effects, indicating that 2-DG suppresses the activation of NLRP3 inflammasomes, as well as the HIF-1 α -NF- κ B pathway in macrophages under OGD conditions.

Discussion

Myocardial infarction stands as one of the deadliest diseases in the world nowadays, posing a significant threat not only to individual lives but also to the vast consumption of healthcare resources. As research delves deeper, the crucial role of the inflammatory myocardial microenvironment in the cardiac repair process has garnered increasing attention^{19,20}. Following MI, the early microenvironment witnesses a raging inflammatory storm, extensive necrosis of myocardial and endothelial cells, and severe impairment of cardiac function. In the later stages, local scarring and myocardial fibrosis mainly involving fibroblasts, along with the formation of ventricular aneurysms, further exacerbate the deterioration of cardiac function^{21–23}. Therefore, effectively modulating the myocardial microenvironment, suppressing the inflammatory storm, and promoting cardiac repair have become hotspots of current research^{24,25}.

The findings from our study elucidate the multifaceted role of the glycolysis inhibitor, 2-DG, delivered via a patch, in modulating inflammatory response in infarcted hearts and cardiac repair post-MI (Fig. 3). The results highlight several key mechanisms by which the 2-DG patch exerts its therapeutic effects, contributing to a nuanced understanding of macrophage metabolism in inflammation and tissue repair.

In this study, the primary observation that 2-DG can inhibit glycolysis in macrophages aligns with previous studies showing the dependency of inflammatory macrophages on glycolytic metabolism^{26,27}. By curbing glycolysis, the 2-DG patch effectively reduces the proinflammatory polarization of macrophages (Fig. 2). This

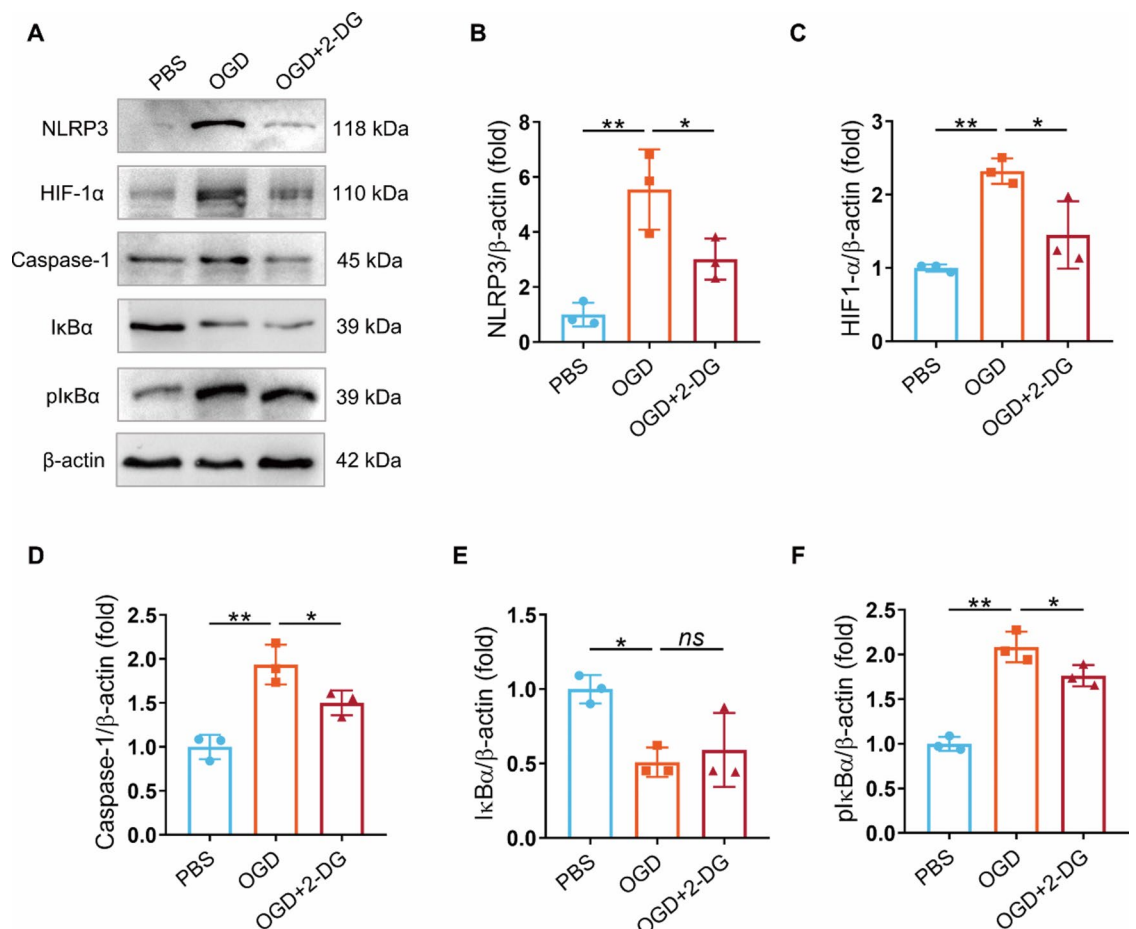


Fig. 6. 2-DG inhibits the NF- κ B pathway and attenuates the activation of inflammasome NLRP3.

Representative images (A) and quantification of western blotting analysis of NLRP3 (B), HIF-1 α (C), Caspase-1 (D), IkBa (E), and pIkBa (F) in macrophages under OGD with or without 2-DG pretreatment. Original blots/gels are presented in Supplementary Figures S6, S7. Error bars represent the SD, and significance was determined using one-way ANOVA followed by Tukey's test (*p < 0.05, **p < 0.01, and ns for not significant).

finding is critical as it underscores the potential of metabolic interventions to modulate immune cell function and inflammatory responses. The diminished proinflammatory activity of macrophages under the influence of 2-DG could be a pivotal factor in mitigating inflammation and fostering a more conducive environment for tissue repair following MI.

One of the most compelling outcomes of our research is the demonstrated ability of the 2-DG patch to facilitate cardiac repair after MI (Fig. 3). The patch's protective effects against the inflammatory response in the infarcted heart are multifaceted. By attenuating the inflammatory response and the infiltration of proinflammatory macrophages into the myocardium (Figs. 4 and 5), the patch helps to preserve cardiac tissue and function. Additionally, the inhibition of the NF- κ B pathway and the attenuation of NLRP3 inflammasome activation are notable mechanisms through which 2-DG confers its anti-inflammatory benefits^{28–30} (Figs. 6 and 7). The suppression of these critical inflammatory pathways suggests that 2-DG not only dampens immediate inflammatory responses but also potentially prevents the chronic inflammatory sequelae that often complicate post-MI recovery.

Our previous study has demonstrated that intraperitoneal injection of 2-DG can improve the myocardial microenvironment, enhancing stem cell retention and subsequently boosting their therapeutic capabilities in MI¹⁵. However, systemic 2-DG injection inevitably brings about certain side effects³¹. To overcome this issue, we designed locally applied 2-DG patch, aiming to capitalize on their positive effects in cardiac repair while avoiding systemic side effects. In the present study, we have demonstrated that the sustained release of 2-DG patch effectively modulates macrophage polarization by regulating glucose metabolism (Figs. 1 and 2). The *in vivo* experiments further elucidated that the therapeutic role of 2-DG patch in cardiac recovery.

Despite the promising results regarding the inhibition of proinflammatory macrophage activity, our study also revealed a limitation of the 2-DG patch: it did not modulate the anti-inflammatory polarization of macrophages either *in vivo* or *in vitro* (Fig. S2). This lack of effect on anti-inflammatory macrophage polarization suggests that while 2-DG effectively suppresses inflammation, it does not promote the alternative activation pathways that could enhance tissue healing and resolution of inflammation. This finding points to a potential area for further research, as combining glycolysis inhibition with other interventions that promote anti-inflammatory macrophage polarization could yield synergistic effects, enhancing overall outcomes in cardiac repair and recovery.

In addition, following MI, the energy supply of cardiomyocytes primarily relies on anaerobic glycolysis, which naturally begs the question: would inhibiting glycolysis with 2-DG induce cardiomyocyte apoptosis? In this case, we exposed H9C2 cells to varying concentrations of 2-DG under hypoxia conditions and explored the apoptosis of cardiomyocytes. As shown in Fig. S5, an appropriate concentration of 2-DG does not cause cardiomyocyte apoptosis, indicating that even under hypoxic condition, when glycolysis is inhibited, cardiomyocytes can still sustain their viability through alternative metabolic pathways, such as amino acid oxidation^{32,33} and ketone body metabolism^{34,35}.

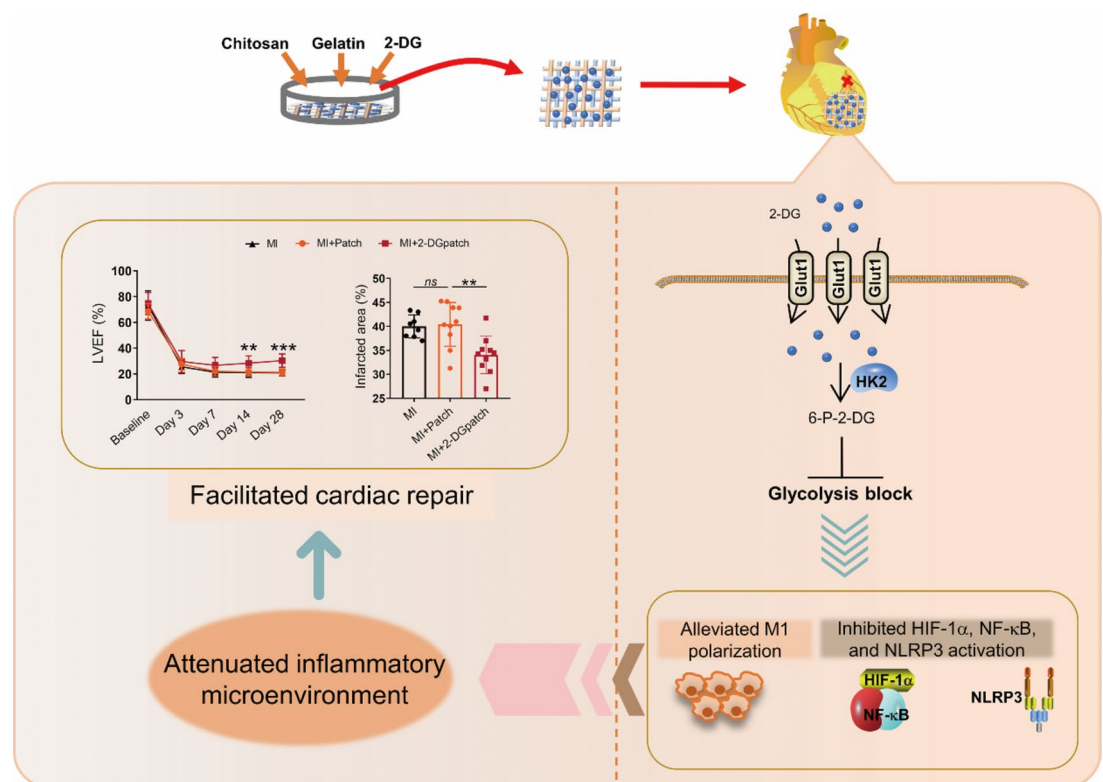


Fig. 7. 2-DG patch facilitated cardiac recovery through attenuating the inflammatory microenvironment in ischemic myocardium.

However, it's crucial to recognize that 2-DG, as a classical glycolytic inhibitor, may pose potential risks due to its non-selectivity. Whether 2-DG exerts toxic effects on other cells *in vivo* remains unknown. Therefore, future studies must delve deeper into the mechanistic actions of 2-DG, aiming to provide a more comprehensive theoretical foundation for its application in the treatment of cardiac diseases.

Conclusion

In conclusion, this study confirms that 2-DG patch can regulate the polarization phenotype of macrophages by inhibiting glycolysis, thereby mitigating inflammatory responses, and promoting cardiac repair following MI. This discovery not only offers a novel perspective on understanding the regulatory mechanisms of the MI micro-environment but also provides robust experimental evidence and theoretical support for developing innovative therapeutic strategies for MI. Nevertheless, we must be mindful of the potential risks and challenges associated with 2-DG as a therapeutic agent. Future research must further explore its mechanism of action and optimize its usage, aiming to maximize its role in the treatment of cardiac diseases.

Methods

Chemicals and reagents

The chitosan and gelatin were purchased from Senopharm (Shanghai, China). 2-DG was purchased from Beyotime (Shanghai, China). Foxp3 fixation/permeation Flow Cytometry Workflow Kit was purchased from Invitrogen (USA). Anti-iNOS antibody (18985-1-AP), anti-IκBα antibody (10268-1-AP), and anti-pIκBα antibody (82319-1-RR) were purchased from Proteintech (USA). Anti-HIF-1α antibody (EP1215Y), anti-NLRP3 antibody (EPR23094-1), and anti-Caspase-1 antibody (EPR16883) were purchased from Abcam (UK). Anti-iNOS-PE (12-5090-82), anti-CD206-APC (17-2160-80), and anti-F4/80-FITC (11-4801-82) were purchased from Invitrogen (USA).

Preparation and characterization of the 2-DG loaded chitosan/gelatin patch

The chitosan/gelatin composite patch loaded with 2-DG was fabricated as we previously described¹⁵. Briefly, after filtration and sterilization, a 4% chitosan (w/v, in 1% acetic acid, Senopharm) and 2% gelatin (w/v, 1% acetic acid, Senopharm) solution were mixed in a weight ratio of 1:1. Then, 1% 2-DG (Beyotime) is added and stirred to ensure complete dissolution. The mixture was centrifuged at 3000–4000 rpm for 15 min to remove impurities and bubbles. The solution was then poured into culture plate and incubated overnight in an oven at 50–66 °C. Afterward, the solution was treated with a 2% NaOH–80% ethanol mixture for 30 min for decarboxylation, and then rinsed with 80% ethanol solution three times, each time for 10 min. Finally, deionized water was added to wash the mixture until it reached neutral pH. The morphology of the composite patch was examined by a scanning electron microscope (SEM, S-4800, Hitachi). The RPMI medium was added to the composite patch and the supernatant (2-DG-CM) was collected 3 days later for *in vitro* analysis.

Cell culture and treatment

Primary peritoneal macrophages were isolated from C57BL/6 mice as we previously reported¹⁵ and cultured in RPMI medium containing 10% FBS (Procell). *In vitro* oxygen–glucose deprivation (OGD) was used to mimic the microenvironment *in vivo* after MI. Briefly, macrophages were cultured in a serum-deprived medium and incubated under hypoxia (1% O₂) for 24 h. In the OGD + 2-DG group, before being transferred into the hypoxic incubation, the culture medium was replaced with 2-DG-CM 3 h in advance to block glycolysis.

Animal study design

All animal procedures were performed in accordance with ARRIVE guidelines and approved by the Ethics Committee of Affiliated Hospital of Nantong University. MI was established on male C57BL/6 mice (8–10 weeks old) as we previously described. Briefly, after general anesthesia, LAD was ligated about 2 mm below the lowest part of the left atrial appendage. Successful ligation was verified by pale left ventricular wall below the ligation site. Mice in the sham group underwent only thoracotomy without LAD ligation. For 2-DG patch group, a prepared 2-DG composite patch was attached to infarct area with fibrin glue (Sigma-Aldrich) immediately after LAD ligation. For single patch group, a chitosan/gelatin patch without 2-DG was attached to the ischemic area. The patch size was approximately 3.5 mm in diameter.

Cardiac single-cell suspensions preparation and flow cytometry analysis

Cardiac single-cell suspension was prepared as described previously, with slight modifications³⁶. Briefly, mice were anesthetized and intracardially perfused with PBS to eliminate blood cells. The hearts were excised, minced with fine scissors, and digested in a Hanks' balanced salt solution-based enzyme solution containing a cocktail of 1 mg/mL type II collagenase (Sigma-Aldrich), 0.5 mg/mL dispase (Sigma-Aldrich), 0.5 mM CaCl₂, and 1 U/mL DNase I (Sigma-Aldrich) for 1 h at 37 °C with oscillation every 15 min. After digestion, samples were filtered with a 70-μm cell strainer. Cells used in subsequent analyses were resuspended and counted after erythrocyte lysis.

For the analysis of cell surface markers, a single-cell suspension was incubated with fluorescently labeled antibodies against cell surface antigens at RT for 30 min. For intracellular marker detection, a Foxp3 fixation/permeation working solution (Invitrogen) was first added at RT for 1 h, and cells were incubated with antibodies for 30 min. Cells were washed and resuspended for flow cytometry (Millipore Guava EasyCyte), as we previously described³⁷. All flowcytometry gates and isotype control were presented in the supplementary data.

Statistical analysis

Statistical analysis was performed using SPSS 25.0 and GraphPad Prism 8 software. The Shapiro–Wilk test was employed to assess the normality of the data. Variables with normal distribution were expressed as mean \pm standard deviation. Significant differences among multiple groups were analyzed using ANOVA followed by Tukey's test. For data that were not normally distributed or had unequal variances, the non-parametric Kruskal–Wallis test was utilized, followed by Dunn's multiple comparison test. To analyze changes in cardiac function over time across multiple groups, a two-way repeated measures ANOVA was conducted, followed by Tukey's test. A p -value < 0.05 was considered statistically significant.

Data availability

All data generated or analyzed during this study are included in this published article (and its Supplementary Information files). Further inquiries can be directed to the corresponding author.

Received: 8 April 2024; Accepted: 28 August 2024

Published online: 02 September 2024

References

1. Yap, J. et al. Macrophages in cardiac remodelling after myocardial infarction. *Nat. Rev. Cardiol.* **20**(6), 373–385 (2023).
2. Tsao, C. W. et al. Heart disease and stroke statistics-2023 update: A report from the American Heart Association. *Circulation* **147**(8), e93–e621 (2023).
3. Reed, G. W., Rossi, J. E. & Cannon, C. P. Acute myocardial infarction. *Lancet* **389**(10065), 197–210 (2017).
4. Widimsky, P., Crea, F., Binder, R. K. & Lüscher, T. F. The year in cardiology 2018: acute coronary syndromes. *Eur. Heart J.* **40**(3), 271–282 (2019).
5. Saito, Y., Oyama, K., Tsujita, K., Yasuda, S. & Kobayashi, Y. Treatment strategies of acute myocardial infarction: Updates on revascularization, pharmacological therapy, and beyond. *J. Cardiol.* **81**(2), 168–178 (2023).
6. Weissman, D. & Maack, C. Mitochondrial function in macrophages controls cardiac repair after myocardial infarction. *J. Clin. Invest.* <https://doi.org/10.1172/JCI167079> (2023).
7. Matter, M. A. et al. Inflammation in acute myocardial infarction: The good, the bad and the ugly. *Eur. Heart J.* **45**(2), 89–103 (2024).
8. Hu, X. et al. A large-scale investigation of hypoxia-preconditioned allogeneic mesenchymal stem cells for myocardial repair in nonhuman primates: Paracrine activity without remuscularization. *Circ. Res.* **118**(6), 970–983 (2016).
9. Peet, C., Ivetic, A., Bromage, D. I. & Shah, A. M. Cardiac monocytes and macrophages after myocardial infarction. *Cardiovasc. Res.* **116**(6), 1101–1112 (2020).
10. Silvis, M. et al. Damage-associated molecular patterns in myocardial infarction and heart transplantation: The road to translational success. *Front. Immunol.* **11**, 599511 (2020).
11. Vafadarnejad, E. et al. Dynamics of cardiac neutrophil diversity in murine myocardial infarction. *Circ. Res.* **127**(9), e232–e249 (2020).
12. Lavine, K. J. et al. The macrophage in cardiac homeostasis and disease: JACC macrophage in CVD series (Part 4). *J. Am. Coll. Cardiol.* **72**(18), 2213–2230 (2018).
13. Kologrivova, I., Shtatolkina, M., Suslova, T. & Ryabov, V. Cells of the immune system in cardiac remodeling: Main players in resolution of inflammation and repair after myocardial infarction. *Front. Immunol.* **12**, 664457 (2021).
14. Mills, E. L. et al. Succinate dehydrogenase supports metabolic repurposing of mitochondria to drive inflammatory macrophages. *Cell* **167**(2), 457–470.e13 (2016).
15. Xiao, W. et al. An immunometabolic patch facilitates mesenchymal stromal/stem cell therapy for myocardial infarction through a macrophage-dependent mechanism. *Bioeng. Transl. Med.* **8**(3), e10471 (2023).
16. Van den Bossche, J. et al. Mitochondrial dysfunction prevents repolarization of inflammatory macrophages. *Cell Rep.* **17**, 684–696 (2016).
17. Mezzaroma, E. et al. The inflammasome promotes adverse cardiac remodeling following acute myocardial infarction in the mouse. *Proc. Natl. Acad. Sci. U. S. A.* **108**(49), 19725–19730 (2011).
18. Xiang, M. et al. Role of oxidative stress in reperfusion following myocardial ischemia and its treatments. *Oxid. Med. Cell Longev.* **2021**, 6614009 (2021).
19. Chen, W. et al. A matrix-metalloproteinase-responsive hydrogel system for modulating the immune microenvironment in myocardial infarction. *Adv. Mater.* **35**(13), e2209041 (2023).
20. Wang, W. et al. Lymphatic endothelial transcription factor Tbx1 promotes an immunosuppressive microenvironment to facilitate post-myocardial infarction repair. *Immunity* **56**(10), 2342–2357.e10 (2023).
21. Prabhu, S. D. & Frangogiannis, N. G. The biological basis for cardiac repair after myocardial infarction: From inflammation to fibrosis. *Circ. Res.* **119**(1), 91–112 (2016).
22. Frangogiannis, N. G. Cardiac fibrosis. *Cardiovasc. Res.* **117**(6), 1450–1488 (2021).
23. Humeres, C. et al. Smad7 effects on TGF- β and ErbB2 restrain myofibroblast activation and protect from postinfarction heart failure. *J. Clin. Invest.* <https://doi.org/10.1172/JCI146926> (2022).
24. Ong, S. B. et al. Inflammation following acute myocardial infarction: Multiple players, dynamic roles, and novel therapeutic opportunities. *Pharmacol. Ther.* **186**, 73–87 (2018).
25. Jia, D. et al. Cardiac resident macrophage-derived legumain improves cardiac repair by promoting clearance and degradation of apoptotic cardiomyocytes after myocardial infarction. *Circulation* **145**(20), 1542–1556 (2022).
26. Zhao, P. et al. Aminoxyacetic acid attenuates post-infarct cardiac dysfunction by balancing macrophage polarization through modulating macrophage metabolism in mice. *J. Cell. Mol. Med.* **24**(4), 2593–2609 (2020).
27. Zhong, W. J. et al. Inhibition of glycolysis alleviates lipopolysaccharide-induced acute lung injury in a mouse model. *J. Cell. Physiol.* **234**(4), 4641–4654 (2019).
28. Zhang, Q. et al. Signaling pathways and targeted therapy for myocardial infarction. *Signal Transduct. Target Ther.* **7**(1), 78 (2022).
29. Abbate, A. et al. Interleukin-1 and the inflammasome as therapeutic targets in cardiovascular disease. *Circ. Res.* **126**(9), 1260–1280 (2020).
30. Derkachev, I. A. et al. Angiotensin 1–7 increases cardiac tolerance to ischemia/reperfusion and mitigates adverse remodeling of the heart-The signaling mechanism. *Fundam. Clin. Pharmacol.* <https://doi.org/10.1111/fcp.12983> (2024).
31. Raez, L. E. et al. A phase I dose-escalation trial of 2-deoxy-D-glucose alone or combined with docetaxel in patients with advanced solid tumors. *Cancer Chemother. Pharmacol.* **71**(2), 523–530 (2013).
32. Weimer, S. et al. D-Glucosamine supplementation extends life span of nematodes and of ageing mice. *Nat. Commun.* **5**, 3563 (2014).
33. Li, T. et al. Defective branched-chain amino acid catabolism disrupts glucose metabolism and sensitizes the heart to ischemia-reperfusion injury. *Cell Metab.* **25**, 374–385 (2017).

34. Selvaraj, S., Kelly, D. P. & Margulies, K. B. Implications of altered ketone metabolism and therapeutic ketosis in heart failure. *Circulation* **141**, 1800–1812 (2020).
35. Puchalska, P. & Crawford, P. A. Multi-dimensional roles of ketone bodies in fuel metabolism, signaling, and therapeutics. *Cell Metab.* **25**, 262–284 (2017).
36. Fan, Q. et al. Dectin-1 contributes to myocardial ischemia/reperfusion injury by regulating macrophage polarization and neutrophil infiltration. *Circulation* **139**(5), 663–678 (2019).
37. Chen, W. et al. Protein phosphatase 2A catalytic subunit α (PP2A α) maintains survival of committed erythroid cells in fetal liver erythropoiesis through the STAT5 pathway. *Am. J. Pathol.* **178**(5), 2333–2343 (2011).

Acknowledgements

This work is supported by the National Natural Science Foundation of China (82370253), Jiangsu Provincial Research Hospital (YJXYY202204), Innovation Team Project of Affiliated Hospital of Nantong University (XNBHCX31773).

Author contributions

Conceptualization, Weizhang Xiao and Jiahai Shi.; Methodology, Weizhang Xiao, Zhen Zhu.; Software, Zhiming Yu and Yue Pan.; Validation, Qun Xue, and Youlang Zhou.; Formal Analysis, Zhiming Yu.; Investigation, Zhen Zhu and Yue Pan.; Resources, Qun Xue, and Youlang Zhou.; Data Curation, Weizhang Xiao.; Writing—Original Draft Preparation, Weizhang Xiao.; Writing—Review & Editing, Jiahai Shi.; Visualization, Youlang Zhou.; Supervision, Youlang Zhou and Jiahai Shi.; Project Administration, Qun Xue and Jiahai Shi.; Funding Acquisition, Weizhang Xiao and Jiahai Shi.

Competing interests

The authors declare no competing interests.

Additional information

Supplementary Information The online version contains supplementary material available at <https://doi.org/10.1038/s41598-024-71473-5>.

Correspondence and requests for materials should be addressed to W.X. or J.S.

Reprints and permissions information is available at www.nature.com/reprints.

Publisher's note Springer Nature remains neutral with regard to jurisdictional claims in published maps and institutional affiliations.

Open Access This article is licensed under a Creative Commons Attribution-NonCommercial-NoDerivatives 4.0 International License, which permits any non-commercial use, sharing, distribution and reproduction in any medium or format, as long as you give appropriate credit to the original author(s) and the source, provide a link to the Creative Commons licence, and indicate if you modified the licensed material. You do not have permission under this licence to share adapted material derived from this article or parts of it. The images or other third party material in this article are included in the article's Creative Commons licence, unless indicated otherwise in a credit line to the material. If material is not included in the article's Creative Commons licence and your intended use is not permitted by statutory regulation or exceeds the permitted use, you will need to obtain permission directly from the copyright holder. To view a copy of this licence, visit <http://creativecommons.org/licenses/by-nc-nd/4.0/>.

© The Author(s) 2024